APPLICATION OF FRACTIONAL CALCULUS TO VISCOELASTICALLY DAMPED STRUCTURES IN THE FINITE ELEMENT METHOD

André Schmidt and Lothar Gaul

Institut A für Mechanik, Universität Stuttgart
Pfaffenwaldring 9, 70550 Stuttgart, Germany

SUMMARY: A generalized rheological element for viscoelasticity, called a 'spring-pot', is deduced by making use of fractional time derivatives. With this new element, fractional differential constitutive equations arise which result in improved curve-fitting properties, especially when experimental data from long time intervals or spanning several frequency decades need to be fitted. Due to the non-locality of fractional derivatives, the computational effort and the storage requirements increase significantly compared to integer-order concepts, when solving the constitutive equations numerically.
In the present work, two spring-pots are used to set up a rheological model for a polymer. The implementation of the resulting fractional constitutive equation into an FE code is demonstrated. Then, a parameter identification in the time domain and in the frequency domain is carried out simultaneously. Finally, FE calcualtions of a viscoelastic member are presented and three different concepts for the reduction of the computational effort and the storage requirements are compared and discussed.

KEYWORDS: viscoelasticity, damping, fractional derivatives, Finite Element Method

INTRODUCTION

It is well-known that all materials show material damping to some extent. When subjected to time periodic loads, a hysteresis can be observed and as a response to a Heaviside step in stress or strain, creep or stress relaxation occurs. The damping properties of some materials, such as rubbers or polymers, are quite pronounced and cannot be neglected when a structure containing these materials is modeled.
Material damping may be modeled by differential operators or hereditary integral viscoelastic constitutive equations. In many applications it is sufficient to use linear viscoelastic stress-strain relations. Usually, linear viscoelasticity is visualized by rheological models, consisting of linear springs and viscous dashpots, which results in constitutive equations of integer-order differential operator type. However, it is known that these models have deficiencies when being applied to large time or frequency intervals.
Improved adaptivity with respect to measured constitutive behavior is obtained by introducing fractional derivatives. The application of fractional derivatives to viscoelasticity was studied substancially by Caputo and Mainardi[5] and is physically founded.[3] This concept results in fractional-order differential stress-strain relations, that provide good curve-fitting properties, require only few parameters and lead to causal behavior.[1,2] Bagley and Torvik[4] derived constraints for the material parameters of the 'fractional 3-parameter model' in order to ensure a non-negative internal work and rate of energy dissipation. Koeller[9] suggested to replace the viscous dashpots in rheological models by generalized elements which he called 'spring-pots'. The resulting constitutive relations then are consistent with thermodynamical principles. An implementation of fractional constitutive equations into FE formulations is given by Padovan.[11] Parameter identifications in the time domain and in the frequency domain for the fractional 3-parameter model in conjunction with 3D FE calculations were presented by Schmidt and Gaul.[13] Enelund and

Josefson[?] studied formulations of hereditary integral type in the FEM. Implementations of fractional constitutive equations in the BEM were investigated by Gaul and Schanz[7] for the time domain and by Gaul[6] for the frequency domain.

GRÜNWALD DEFINITION OF FRACTIONAL DERIVATIVES

Starting point is the definition of the first (integer order) time derivative in terms of a backward difference quotient

$$\frac{\mathrm{d}^1 f(t)}{\mathrm{d}t^1} = \lim_{\Delta t \to 0} \frac{1}{\Delta t} \left[f(t) - f(t - \Delta t) \right] . \tag{1}$$

Repeated application leads to

$$\frac{\mathrm{d}^2 f(t)}{\mathrm{d}t^2} = \lim_{\Delta t \to 0} \frac{1}{(\Delta t)^2} \left[f(t) - 2f(t - \Delta t) + f(t - 2\Delta t) \right] , \tag{2}$$

$$\frac{\mathrm{d}^3 f(t)}{\mathrm{d}t^3} = \lim_{\Delta t \to 0} \frac{1}{(\Delta t)^3} \left[f(t) - 3f(t - \Delta t) + 3f(t - 2\Delta t) - f(t - 3\Delta t) \right] , \tag{3}$$

etc. Thus, any integer-order derivative is given by

$$\frac{\mathrm{d}^n f(t)}{\mathrm{d}t^n} = \lim_{\Delta t \to 0} \left[\frac{1}{(\Delta t)^n} \sum_{j=0}^{n} (-1)^j \left(\begin{array}{c} n \\ j \end{array} \right) f(t - j\Delta t) \right] \tag{4}$$

where the binomial coefficient $\left(\begin{array}{c} n \\ j \end{array} \right)$ is used. If we replace the time step Δt by the fraction $\frac{t}{N}$, such that $N = 1, 2, 3, ...$, Eqn 4 can be written as

$$\frac{\mathrm{d}^n f(t)}{\mathrm{d}t^n} = \lim_{N \to \infty} \left[\left(\frac{t}{N} \right)^{-n} \sum_{j=0}^{N-1} (-1)^j \left(\begin{array}{c} n \\ j \end{array} \right) f(t - j\tfrac{t}{N}) \right] \tag{5}$$

noting that

$$\left(\begin{array}{c} n \\ j \end{array} \right) = 0 \qquad \text{for} \quad j > n . \tag{6}$$

The upper limit of the sum $N - 1$ seems to be somewhat arbitrary. However, it derives from defining the lower limit of an integral, when Eqn 5 is used to define integrals as a limit of a Riemann sum, see Oldham and Spanier[10] or Podlubny.[12]
In order to deduce a formulation that is valid for any real order derivative, we use the extended definition of the binomial coefficient

$$\left(\begin{array}{c} a \\ j \end{array} \right) = \begin{cases} \frac{a(a-1)(a-2)\cdots(a-j+1)}{j} & \text{for} \quad j > 0 \\ 1 & \text{for} \quad j = 0 \end{cases} \tag{7}$$

wherein a is real and j is a natural number. For $j > 0$ the expression $(-1)^j \left(\begin{array}{c} n \\ j \end{array} \right)$ can then be written as

$$\begin{aligned} (-1)^j \left(\begin{array}{c} n \\ j \end{array} \right) &= (-1)^j \frac{\overbrace{n(n-1)(n-2)\cdots(n-j+2)(n-j+1)}^{\text{j factors}}}{j!} \\ &= \frac{(j-n-1)(j-n-2)\cdots(-n+1)(-n)}{j!} = \left(\begin{array}{c} j-n-1 \\ j \end{array} \right) \equiv \frac{\Gamma(j-n)}{\Gamma(-n)\Gamma(j+1)} \end{aligned} \tag{8}$$

such that Γ is the gamma function. For $j = 0$ Eqn 8 of course holds as well. Inserting Eqn 8 into Eqn 5, we obtain

$$\frac{\mathrm{d}^n f(t)}{\mathrm{d}t^n} = \lim_{N \to \infty} \left[\left(\frac{t}{N} \right)^{-n} \sum_{j=0}^{N-1} \frac{\Gamma(j-n)}{\Gamma(-n)\Gamma(j+1)} \, f(t - j\tfrac{t}{N}) \right] \tag{9}$$

which is valid for all integer-order derivatives ($n > 0$). If we now reinterpret n to be any real number ν, the Grünwald definition of fractional derivatives and integrals[8] is derived

$$\frac{\mathrm{d}^\nu f(t)}{\mathrm{d}t^\nu} = \lim_{N\to\infty}\left[\left(\frac{t}{N}\right)^{-\nu}\sum_{j=0}^{N-1} A_{j+1}\; f(t-j\,\tfrac{t}{N})\right] \;, \tag{10}$$

where

$$A_{j+1} \equiv \frac{\Gamma(j-\nu)}{\Gamma(-\nu)\Gamma(j+1)} \tag{11}$$

are the so-called Grünwald coefficients A_{j+1}.

Note in this context, that all Grünwald coefficients A_{j+1} are different from zero as long as the order of derivative ν is not a positive integer. If, e.g. $\nu = -1$, then $A_{j+1} = 1$ for all j, according to the Riemann sum for integer-order integration.
For ν being a natural number n, only the first $n+1$ Grünwald coefficients A_{j+1} are non-zero, indicating a local operator. On the other hand, since for any positive non-integer number all coefficients A_{j+1} are non-zero, fractional derivatives are non-local operators (except for integer-order derivatives). Analogous to the integer-order integral, the lower limit (also called 'terminal') of the fractional derivative in Eqn 10 is zero. This is indicated by the function values taken into account in the sum in Eqn 10, i.e. the first addend ($j = 0$) is $A_1 f(t)$ and the last ($j = N-1$) is $A_N f(t - \frac{N-1}{N}t) = A_N f(\frac{t}{N})$. Thus, the interval $(0, t]$ is divided into N sections of equal size for the calculation of the fractional derivative or integral.
In this paper the lower terminal is assumed to be zero. This may be indicated using the differential operator representation

$${}_0\mathrm{D}_t^\nu\, f(t) \;=\; \frac{\mathrm{d}^\nu f(t)}{\mathrm{d}t^\nu} \;=\; \lim_{N\to\infty}\left[\left(\frac{t}{N}\right)^{-\nu}\sum_{j=0}^{N-1} A_{j+1}\, f(t-j\,\tfrac{t}{N})\right] \tag{12}$$

such that the lower indices 0 and t indicate the lower and upper terminal of the fractional differential operator, respectively. In what follows, the lower indices are skipped, hence $\mathrm{D}^\nu = {}_0\mathrm{D}_t^\nu$.

NUMERICAL CALCULATION OF FRACTIONAL DERIVATIVES

Analogous to the numerical evaluation of integrals, fractional derivatives can be calculated by approximating the infinite sum in Eqn 10 by a finite sum, such that $N < \infty$,

$$\mathrm{D}^\nu\, f(t) \approx \left(\frac{t}{N}\right)^{-\nu}\sum_{j=0}^{N-1} A_{j+1}\, f(t-j\,\tfrac{t}{N}) \;. \tag{13}$$

When calculating the Grünwald coefficients A_{j+1} by Eqn 11, numerical problems can arise if ν is close to an integer or if large values of j occur. Therefore, the calculation of the Grünwald coefficients A_{j+1} should be realized by the recursive relationship

$$A_{j+1} \;=\; \frac{\Gamma(j-\nu)}{\Gamma(-\nu)\Gamma(j+1)} \;=\; \frac{j-1-\nu}{j}\,\frac{\Gamma(j-1-\nu)}{\Gamma(-\nu)\Gamma(j)} \;=\; \frac{j-1-\nu}{j}\; A_j \;. \tag{14}$$

One can show that the series given by $|A_{j+1}|$ is strictly decreasing for all $j > \nu$ and that it tends to zero

$$\lim_{j\to\infty} |A_{j+1}| \;=\; 0 \;, \tag{15}$$

see Schmidt and Gaul.[13] With growing j the Grünwald coefficients are weighting function values that are situated further in the past. This is why the influence of the past is faded out as time elapses, which is attributed to the 'fading memory' property.

In the section 'Finite Element Formulation and Implementation', fractional derivatives will be used in conjunction with a time integration algorithm, where fractional derivatives have to be computed at each increment. The time-discrete function values $f(t - j\,\frac{t}{N})$ that are needed to evaluate the fractional

derivative are then computed from the history of the time integration. Usually, the time step size for the evaluation of the fractional derivative $\frac{t}{N}$ is taken equal to the time step size for time integration Δt. Thus, at the beginning of time integration $t = 0$ there is no history ($N = 1$), but the more time increments are calculated, the more history has to be taken into consideration and the computation of the fractional derivative slows down. In addition, the storage requirements increase, as the whole history must be saved. In the following, three different concepts are presented in order to speed up the calculation and to reduce the storage requirements.

Concept A

The property of the 'fading memory' in Eqn 15 motivates the truncation of the history in Eqn 13:

$$\mathrm{D}^{\nu} f(t) \approx \left(\frac{t}{N}\right)^{-\nu} \sum_{j=0}^{N_\ell} A_{j+1}\, f(t - j\tfrac{t}{N}) \;, \qquad N_\ell > N - 1 \tag{16}$$

such that only up to N_ℓ sample points of the past $f(t - j\frac{t}{N})$ are under consideration. Hence, during time integration the numerical effort is the same as with Eqn 13, until all N_ℓ sample points are needed. Then, for each new sample point, the oldest one drops out and the numerical effort as well as the storage requirements stay constant for the rest of time integration.

Concept B

Another possibility to reduce the numerical effort is to choose the step size $\frac{t}{N}$ for the evaluation of the fractional derivative as a multiple of the time step size Δt for time integration

$$\frac{t}{N} \;=\; c\;\Delta t \;, \qquad c > 1 \;. \tag{17}$$

If, e.g. $c = 2$, the number of sample points $f(t - j\frac{t}{N})$ to be considered when calculating the fractional derivative in each time increment is reduced by a factor of 2. In addition, only in every second time increment the fractional derivative has to be calculated and the storage requirements bisect.
As with growing c the level of accuracy of the fractional derivative in Eqn 13 is decreasing, there is a limit for selecting c. On the other hand, investigations have shown that the requirements for the time step size Δt are higher than those for the time step size $\frac{t}{N}$ in order to ensure some desired degree of accuracy, see eg. Padovan.[11] Therefore, a moderate factor, e.g. $c = 2$ seems to be justified.

Concept C

The idea behind this concept is to take the 'newer' history into consideration with a high resolution and the older one with a low resolution, instead of truncating it as in concept A. Starting point is the approximation in Eqn 13. Using the recursive relation in Eqn 14, we obtain at time t_0

$$\begin{aligned} \mathrm{D}^{\nu} f(t) \;\approx\; \left(\frac{t_0}{N}\right)^{-\nu} & \left[\sum_{j=0}^{i} A_{j+1}\, f_j + A_{i+2}\left(f_{i+1} + \tfrac{i-\nu+1}{i+2}\, f_{i+2} + \tfrac{(i-\nu+1)(i-\nu+2)}{(i+2)(i+3)}\, f_{i+3} + \cdots\right)\right] \\ & \stackrel{!}{=} \left(\frac{t_0}{N}\right)^{-\nu} \left[\sum_{j=0}^{i} A_{j+1}\, f_j + A_{i+2}\, T_{i+1}\right] \;, \end{aligned} \tag{18}$$

where f_j is an abbreviation for $f(t_0 - j\frac{t_0}{N})$. Now, we consider the expression T_{i+1} which represents a whole interval as *one* contribution to the fractional derivative, see Fig. 1. The upper limit $t_0 - (i+1)\frac{t_0}{N}$ and lower limit shall be constant during time integration, i.e. $i = \text{const}$. Thus, n time increments later at time $t_0 + n\,\Delta t$ the fractional derivative is given by

$$\begin{aligned} \mathrm{D}^{\nu} f(t) \;\approx\; \left(\frac{t_0}{N}\right)^{-\nu} & \left[\sum_{j=0}^{i+n} A_{j+1}\, f_{j-n} + A_{i+n+2}\left(f_{i+1} + \tfrac{i+n-\nu+1}{i+n+2}\, f_{i+2} + \tfrac{(i+n-\nu+1)(i+n-\nu+2)}{(i+n+2)(i+n+3)}\, f_{i+3} + \cdots\right)\right] \\ & = \left(\frac{t_0}{N}\right)^{-\nu} \left[\sum_{j=0}^{i+n} A_{j+1}\, f_{j-n} + A_{i+n+2}\, T_{i+n+1}\right] \;. \end{aligned} \tag{19}$$

Fig. 1: *Time axis; definition of the interval*

When applying the concept of fractional derivatives to viscoelasticity, the orders of fractional derivatives ν are positive. Thus, for $i > \nu - 1$ we see from Eqns 18 and 19 that the value of all weighting factors in T ranges between zero and unity. In addition, as time elapses, all weighting factors are strictly increasing and tend to unity. Simultaneously, the weighting factor of T tends to zero, such that the influence of the interval under consideration is fading out.

Knowing the 'starting value' T_{i+1} at the time t_0 and the value T_∞ for $t \to \infty$, we can approximate the time dependent value T_{i+n+1}, using the unity function $f^{\mathbf{1}} = 1$:

$$T_{i+n+1} \;=\; T_{i+1} \;+\; \frac{T^{\mathbf{1}}_{i+n+1} - T^{\mathbf{1}}_{i+1}}{T^{\mathbf{1}}_{\infty} - T^{\mathbf{1}}_{i+1}} \,(T_\infty - T_{i+1}) \quad \stackrel{!}{=} \quad T_{i+1} \;+\; w_{i+n+1}(T_\infty - T_{i+1}) \;, \tag{20}$$

where the upper-right index in bold face indicates that the variable is evaluated with the unity function.

The advantage of this concept comes into operation when it is applied to spatially discretized structures like in the FEM. As we will see in the next section, fractional derivatives of stresses and strains have to be evaluated. Thus, the fractional derivatives are needed for all nodal displacements and the stresses at all integration points. Since the weighting factor w_{i+n+1} only depends on time, it can be calculated once at the beginning of each increment. Then it can be used for the calculation of all needed fractional derivatives. For each nodal displacement and stress state at each integration point, only the values of T_{i+1} and T_∞ have to be calculated and stored in order to approximate the influence of the time interval under consideration on the fractional derivative. Note, concept C is not restricted to only one interval. For calculations whith a high number of time increments, many intervals can be established sucessively.

The quality of approximation Eqn 20 is demonstrated by applying it to three different functions

$$f_1(t) = 1 \;, \qquad f_2(t) = a\,t \;, \qquad f_3(t) = \sin(\pi\, a\, t) \qquad \text{where} \qquad a = \frac{1}{\mathrm{s}} \tag{21}$$

and comparing it to Eqn 13. The time interval under consideration ranges from $0\,\mathrm{s}$ to $1\,\mathrm{s}$ and the time step sizes are chosen to be $\frac{t_0}{N} = \Delta t = 0.05\,\mathrm{s}$. The number i of time increments is $i = 20$ such that $t_0 = 2\,\mathrm{s}$. The order of derivative is set to $\nu = 0.5$, which is a typical value for viscoelastic material. The value of T is then computed for the next 500 time increments. In Fig. 2, at the top the functions f_i are displayed in the interval $[0\,\mathrm{s},\, 1\,\mathrm{s}]$. At the bottom, the time depending value of T_{i+n+1} is displayed as a solid line for Eqn 19 and as a dashed line for the approximation in Eqn 20.

As expected, for the constant function f_1 the approximations in Eqns 19 and 20 yield the same results. The second and third example show that approximation 20 provides the same results as Eqn 19 for $t = t_0$ and for $t \to \infty$. For any time $t \in (t_0, \infty)$, there is some moderate deviation which does not exceed $1,1\%$ in our examples.

FRACTIONAL-ORDER CONSTITUTIVE EQUATION

Usually, rheological models of linear viscoelasticity consist of springs and dashpots. The constitutive equations of these elements may be generalized (see Fig. 3) using fractional derivatives. The resulting fractional constitutive equation

$$\sigma \;=\; p\,\mathrm{D}^{\nu}\,\varepsilon \tag{22}$$

includes p as a proportionality factor and ν as the order of derivative which is commonly taken to range between 0 and 1. If $\nu = 0$, Eqn (22) describes the behavior of a spring where p specifies the springs'

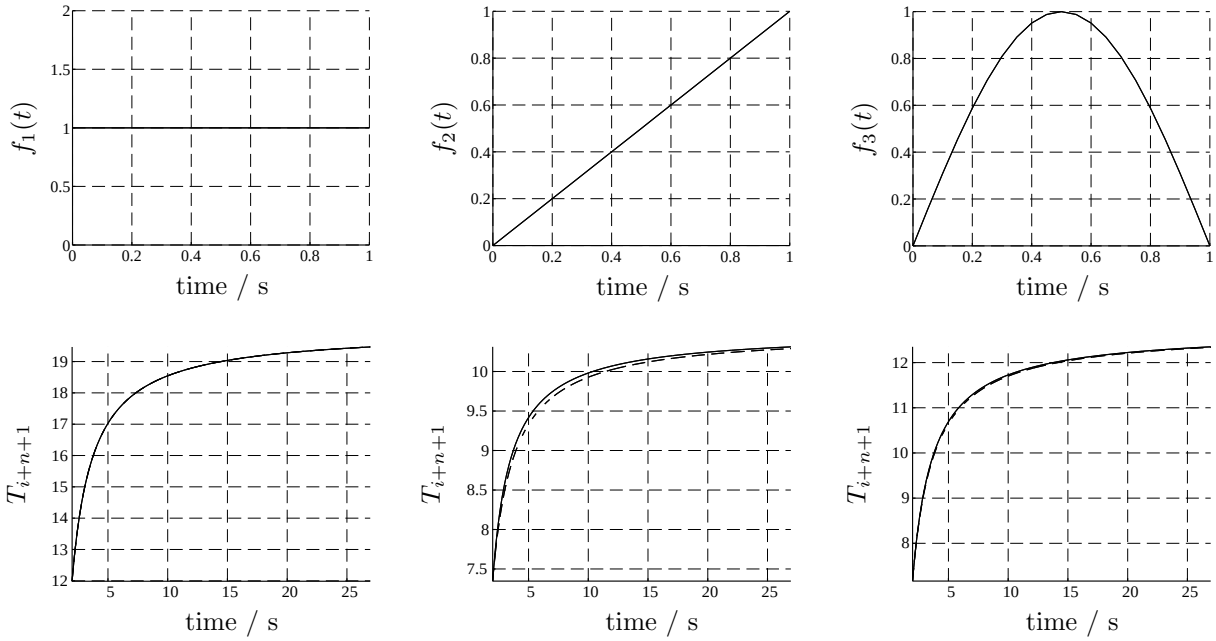

Fig. 2: *Approximation of fractional derivatives, concept C*

stiffness. For $\nu = 1$, Eqn 22 defines the constitutive equation of a dashpot, in which p defines the viscosity. Thus, the fractional constitutive equation 22 'interpolates' between the material behavior of a spring and that of a dashpot. The rheological element which refers to Eqn 22 was therefore introduced by Koeller[9] as a 'spring-pot' and is denoted by a rhomb, see Fig. 3.

By replacing the dashpots in rheological models by spring-pots, fractional rheological models are derived. Application to the 5-parameter model (two Maxwell elements and a spring in parallel) results in the 'fractional 5-parameter model', see Fig. 4. Its constitutive equation is given by

$$\begin{aligned} \sigma + \frac{p_1}{E_1}\,\mathrm{D}^{\nu_1}\sigma + \frac{p_2}{E_2}\,\mathrm{D}^{\nu_2}\sigma + \frac{p_1 p_2}{E_1 E_2}\,\mathrm{D}^{\nu_1+\nu_2}\sigma \\ = E_0\varepsilon + p_1\frac{E_0+E_1}{E_1}\,\mathrm{D}^{\nu_1}\varepsilon + p_2\frac{E_0+E_2}{E_2}\,\mathrm{D}^{\nu_2}\varepsilon + p_1 p_2\frac{E_0+E_1+E_2}{E_1 E_2}\,\mathrm{D}^{\nu_1+\nu_2}\varepsilon\ . \end{aligned} \tag{23}$$

For the solution of this fractional differential equation, pertinent fractional-order initial conditions have to be defined. In this paper, all initial conditions are assumed to be zero, refering to a material that is completely relaxed at $t = 0$.

An extension of Eqn 23 to three dimensions, differentiating between the hydrostatic and the deviatoric states is demonstrated by Schmidt and Gaul[13] for isotropic materials. In this work, we restrict ourselves to the one-dimensional case.

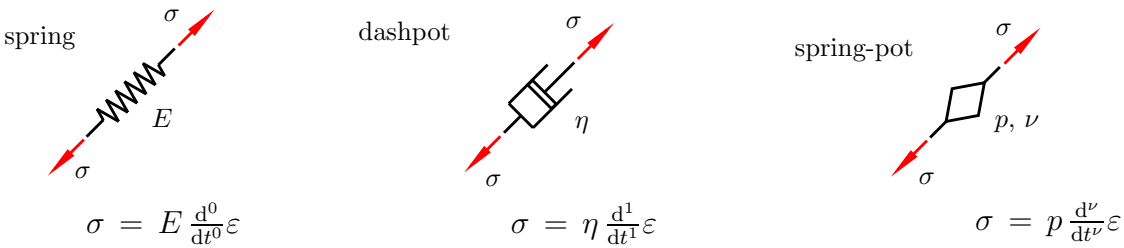

Fig. 3: Rheological elements of viscoelasticity

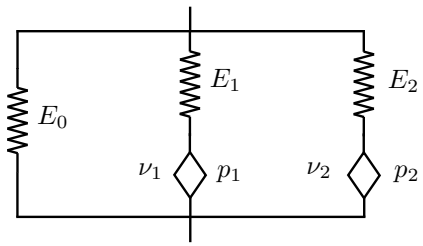

Fig. 4: Fractional 5-parameter model

FINITE ELEMENT FORMULATION AND IMPLEMENTATION

The displacement type formulation for the Finite Element Method is based on

$$\boldsymbol{u} \;=\; \boldsymbol{H}\,\hat{\boldsymbol{u}}\;, \tag{24}$$

where $\boldsymbol{u}$ denotes the displacement field of an element, $\hat{\boldsymbol{u}}$ is the vector of the nodal displacements and $\boldsymbol{H}$ specifies the shape functions. The strain field $\boldsymbol{\varepsilon}$ and the nodal displacements are linked by

$$\boldsymbol{\varepsilon} \;=\; \boldsymbol{B}\,\hat{\boldsymbol{u}}\;, \tag{25}$$

such that $\boldsymbol{B}$ defines the appropriate spatial derivatives of $\boldsymbol{H}$. The principle of virtual work yields the equation of motion

$$\int_R \boldsymbol{B}^T\boldsymbol{\sigma}\;\mathrm{d}R + \boldsymbol{M}\,\ddot{\hat{\boldsymbol{u}}} \;=\; \boldsymbol{r} \tag{26}$$

where R is the region in which the element is defined and $\boldsymbol{r}$ defines the external and the body forces. The consistent mass matrix $\boldsymbol{M}$ is given by

$$\boldsymbol{M} \;=\; \int_R \boldsymbol{H}^T\rho\boldsymbol{H}\;\mathrm{d}R\;, \tag{27}$$

ρ denoting the mass density of the material. To simplify matters, in the following the accent $\hat{\cdot}$ is skipped. At time t, indexed on the upper-left of the variable, the equation of motion results in

$$\int_V \boldsymbol{B}^T\;{}^t\boldsymbol{\sigma}\;\mathrm{d}R + \boldsymbol{M}\;{}^t\ddot{\boldsymbol{u}} \;=\; {}^t\boldsymbol{r}\;. \tag{28}$$

The stress vector ${}^t\boldsymbol{\sigma}$ is derived from the viscoelastic constitutive equation (23). If we apply the time discrete Grünwaldian formulation of fractional derivatives (16) to Eqn (23) and solve for ${}^t\boldsymbol{\sigma}$, we obtain

$$\begin{aligned}
{}^t\boldsymbol{\sigma} \;=\; &\left[1 + \frac{p_1}{E_1}A_1^{(\nu_1)}\left(\frac{t}{N}\right)^{-\nu_1} + \frac{p_2}{E_2}A_1^{(\nu_2)}\left(\frac{t}{N}\right)^{-\nu_2} + \frac{p_1p_2}{E_1E_2}A_1^{(\nu_1+\nu_2)}\left(\frac{t}{N}\right)^{-\nu_1-\nu_2}\right]^{-1}\cdot\\
&\left[E_0\,{}^t\boldsymbol{\varepsilon} + p_1\frac{E_0+E_1}{E_1}\left(\frac{t}{N}\right)^{-\nu_1}\sum_{j=0}^{N}A_{j+1}^{(\nu_1)\;t-j\frac{t}{N}}\boldsymbol{\varepsilon} + p_2\frac{E_0+E_2}{E_2}\left(\frac{t}{N}\right)^{-\nu_2}\sum_{j=0}^{N}A_{j+1}^{(\nu_2)\;t-j\frac{t}{N}}\boldsymbol{\varepsilon}\right.\\
&+ p_1p_2\frac{E_0+E_1+E_2}{E_1E_2}\left(\frac{t}{N}\right)^{-\nu_1-\nu_2}\sum_{j=0}^{N}A_{j+1}^{(\nu_1+\nu_2)\;t-j\frac{t}{N}}\boldsymbol{\varepsilon} - \frac{p_1}{E_1}\left(\frac{t}{N}\right)^{-\nu_1}\sum_{j=1}^{N}A_{j+1}^{(\nu_1)\;t-j\frac{t}{N}}\boldsymbol{\sigma}\\
&\left.- \frac{p_2}{E_2}\left(\frac{t}{N}\right)^{-\nu_2}\sum_{j=1}^{N}A_{j+1}^{(\nu_2)\;t-j\frac{t}{N}}\boldsymbol{\sigma} - \frac{p_1p_2}{E_1E_2}\left(\frac{t}{N}\right)^{-\nu_1-\nu_2}\sum_{j=1}^{N}A_{j+1}^{(\nu_1+\nu_2)\;t-j\frac{t}{N}}\boldsymbol{\sigma}\right]\;,
\end{aligned} \tag{29}$$

where the upper-right indices in brackets indicate the dependance of the Grünwald coefficients on the order of respective fractional derivative. Note, Eqn 29 depends on the actual strain, the strain history and the stress history. If we insert Eqn 29 into Eqn 28 and replace the strains $\boldsymbol{\varepsilon}$ by relation 25, the resulting equation of motion can be transformed into

$$\boldsymbol{M}\;{}^t\ddot{\boldsymbol{u}} + \boldsymbol{K}^*\boldsymbol{u} \;=\; {}^t\boldsymbol{r}^*\;, \tag{30}$$

such that $\boldsymbol{K}^*$ is a modified stiffness matrix and $\boldsymbol{r}^*$ is a modified force vector which contains the effects of the strain and the stress history, see Schmidt and Gaul.[13] Regarding the form of Eqn 30, it can be solved with any elastic FE solver in conjunction with either implicit and explicit integration schemes.

PARAMETER IDENTIFICATION

A parameter identification for the polymer Delrin$^{\mathrm{TM}}$ is carried out in the time domain and in the frequency domain simultaneously. The time-dependant behavior is given in terms of the creep modulus E_c in the range from $10\,\mathrm{s}$ up to $10\,000\,\mathrm{h}$. Besides the measurements of the manufacturer, own measurements have been carried out to cover the short-time period smaller than $360\,\mathrm{s}$. In addition, free decay tests of a cantilever made of Delrin$^{\mathrm{TM}}$ have been carried out at 12 different frequencies in the range from $50\,\mathrm{Hz}$ up to $500\,\mathrm{Hz}$. The oscillations were measured by a laser vibrometer and the frequency-dependant complex modulus was calculated.
The 7 material parameters of the fractional 5-parameter model (see Fig. 4) are identified in terms of an optimization using the least-square fit method. While the complex modulus of the fractional rheological models can be calculated analytically (see Schmidt and Gaul[13]), the time-dependant behavior is evaluated by numerical time integration in each iteration step. The material parameters are given in Table 1 while the time and frequency dependent material behavior is compared to the measurements in Fig. 5.

Table 1: Identified parameters in the time and frequency domain

E_0	E_1	E_2	p_1	p_2	ν_1	ν_2
$58.534\,\frac{\mathrm{N}}{\mathrm{mm}^2}$	$2760.8\,\frac{\mathrm{N}}{\mathrm{mm}^2}$	$2967.7\,\frac{\mathrm{N}}{\mathrm{mm}^2}$	$24.797\,\frac{\mathrm{N}}{\mathrm{mm}^2}\,\mathrm{s}^{\nu_1}$	$62\,510\,\frac{\mathrm{N}}{\mathrm{mm}^2}\,\mathrm{s}^{\nu_2}$	0.19911	0.24991

FE CALCULATION AND COMPARISON OF THE DIFFERENT CONCEPTS

An implementation into the FE code MARC is realized according to the section 'Finite Element Formulation and Implementation' for isoparametric 8-noded brick elements. In addition, the concepts A, B and C are available in order to decrease the numerical costs.
As an example, the free decay of a cantilever made of Delrin$^{\mathrm{TM}}$ is calculated, where the identified fractional 5-parameter model (see section above) is used. The FE model is shown in Fig. 6. At the left side, fixed displacement typ of boundary conditions are applied to the first 2 rows of nodes in order to model the fixed support. The free length of the cantilever is $100\,\mathrm{mm}$, while its cross-section measures $2.2\,\mathrm{mm} \times 10\,\mathrm{mm}$. The model is initially at rest and in the first increment, a steady force in y-direction is applied to the last row of nodes at the right-hand side. Thus, an oscillation about the position of equilibrium is excited, while the position of equilibrium moves with time due to material creep. Since the height of the model has no influence on either the vibration and the creep, only one row of elements is modeled. The calculation is continued for 2000 time increments of $0.001\,\mathrm{s}$ using the Newmark integra-

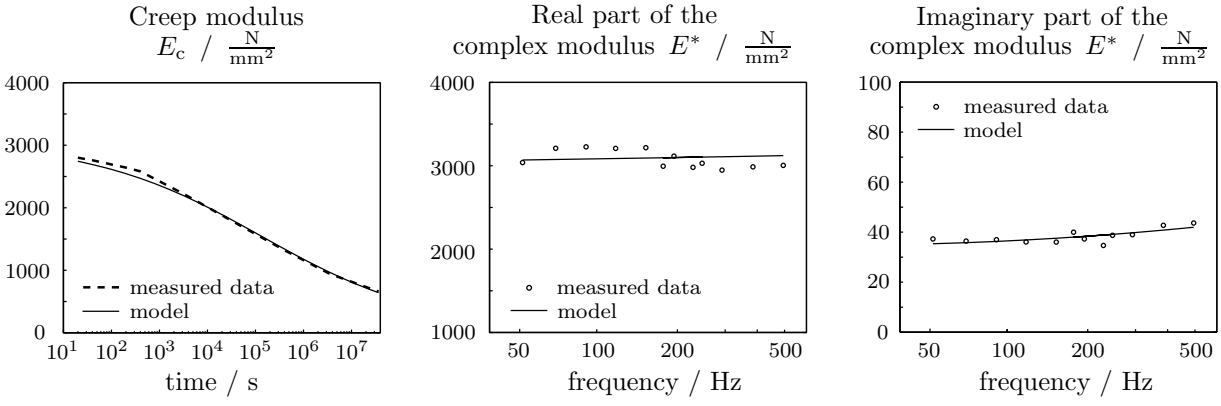

Fig. 5: Comparison between measured data and fractional 5-parameter model

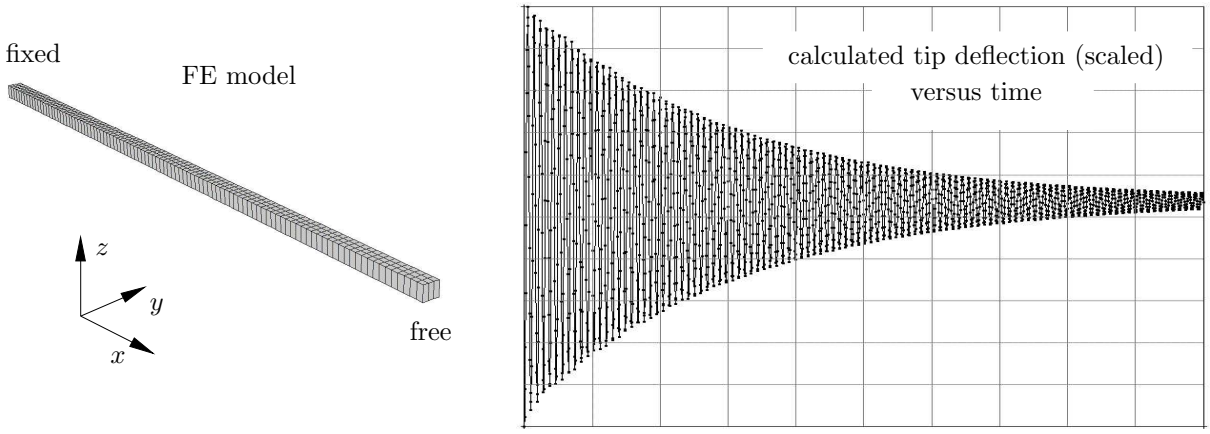

Fig. 6: FE model and calculated tip deflection

tion scheme without numerical damping. Calculations are performed with the 'original' approximation of fractional derivatives (Eqn 13) as the 'reference calculation' and with the conceps A, B and C. The results of the decaying oscillation can be compared to the respective measurements, while the superposed creep behavior can be compared to the theoretical curve from numerical integration (see section above).

The tip deflection of the cantilever is given exemplarily for the reference calculation in Fig. 6. The reference calculation and the concepts A and C fit the measured frequency and the decaying behavior of the cantilever quite well. With concept B, numerical instabilities occur such that only during the first few hundred increments the results are fairly accurat. The needed cpu-time and the storage requirements are given in Table 2 together with a specification of the parameters of the different concepts.

Table 2: Comparison of the computational requirements for the different concepts

	ref. calculation	concept A	concept B	concept C
parameters	—	$N_\ell = 250$	$c = 2$	$i = 50$, length of intervals: $200\,\frac{t}{N}$
relative cpu-time	100 %	24.43 %	26.60 %	24.70 %
relative memory	100 %	18.56 %	53.88 %	26.25 %

Further deviations of the different concepts can be seen from the creep behavior. Since the state of equilibrium can not be extracted directly from the calculation, the mean values of each two consecutive maxima are calculated and a polynomial is fitted. The resulting creep curves are displayed in Fig. 7. While the creep curves of the reference calculation and the concepts B and C are indistinguishable, concept A shows significant deviation. The reason for this inaccuracy is the fact that the creep properties are affected by the whole deformation history. Thus, as with concept A only the newest part of the history is under consideration, after N_ℓ time increments the errors accumulate during time integration.

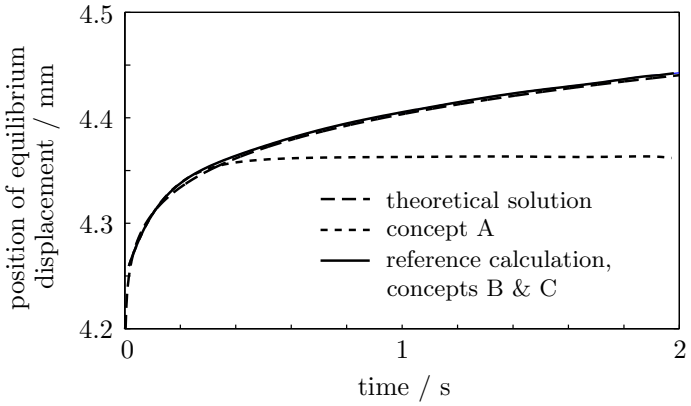

Fig. 7: creep behavior of the cantilever

CONCLUSIONS

In this work, fractional time derivatives were used to deduce a new, generalized rheological element, called a 'spring-pot'. If one replaces the dash-pots in traditional rheological models by spring-pots, gereralized models of linear viscoelasticity are obtained. The constitutive equations of these models were shown to be differential equations of fractional order which can be used in conjunction with FE formulations, using the time discrete Grünwald definition of fractional derivatives. A parameter identification for a polymer in the time and in the frequency domain simultaneously pointed out the excellent adaptivity of this concept to measured data over broad ranges of both time and frequency. The main disadvantage of this method is the increasing numerical effort and the storage requirements due to the non-locality of fractional operators. Thus, three different concepts A, B and C were presented in order to reduce the computational requirements. As long as pure oscillations are under consideration, concepts A and C result in an substancial decrease of the numerical costs, retaining a high level of accuracy. With concept B, numerical instabilities arise, resulting in significant inaccuracies to after some hundred time increments. If creep processes are examined, the whole history has to be taken under consideration. Thus, with concept A obvious deviations occur which can be prevented by using concept B or C instead. Hence, only with concept C substantial reduction of the numerical effort can be achieved without losing accuracy for both, the oscillation behavior and the creep properties.

REFERENCES

1. Bagley, R. L.; Torvik, P. J.: A generalized derivative model for an elastomer damper. Shock and Vibration Bulletin 49 (1979), S. 135–143.

2. Bagley, R. L.; Torvik, P. J.: Fractional calculus — a different approach to the analysis of viscoelastically damped structures. AIAA Journal 21 (1983), Nr. 5, S. 741–748.

3. Bagley, R. L.; Torvik, P. J.: A theoretical basis for the application of fractional calculus to viscoelasticity. Journal of Rheology 27 (1983), Nr. 3, S. 201–210.

4. Bagley, R. L.; Torvik, P. J.: On the fractional calculus model of viscoelastic behavior. Journal of Rheology 30 (1986), Nr. 1, S. 133–155.

5. Caputo, M.; Mainardi, F.: Linear models of dissipation in anelastic solids. Rivista del Nuovo Cimento 1 (1971), Nr. 2, S. 161–198.

6. Gaul, L.: The influence of damping on waves and vibrations. Mechanical Systems and Signal Processing 13 (1999), Nr. 1, S. 1–30.

7. Gaul, L.; Schanz, M.: A comparative study of three boundary element approaches to calculate the transient response of viscoelastic solids with unbounded domains. Comput. Methods Appl. Mech. Engrg. 179 (1999), S. 111–123.

8. Grünwald, A. K.: Über 'begrenzte' Derivationen und deren Anwendung. Zeitschrift für angewandte Mathematik und Physik 12 (1867), S. 441–480.

9. Koeller, R. C.: Application of fractional calculus to the theory of viscoelasticity. Journal of Applied Mechanics 51 (1984), S. 299–307.

10. Oldham, K. B.; Spanier, J.: The Fractional Calculus. Academic Press, New York and London, 1974.

11. Padovan, J.: Computational algorithms for FE formulations involving fractional operators. Computational Mechanics 2 (1987), S. 271–287.

12. Podlubny, I.: Fractional Differential Equations. Academic Press, San Diego and London, 1999.

13. Schmidt, A.; Gaul, L.: FE implementation of viscoelastic constitutive stress-strain relations involving fractional time derivatives. In: Constitutive Models for Rubber II. A.A.Balkema Publishers, Tokyo, 2001, S. 79–89.